Since January 2020 Elsevier has created a COVID-19 resource centre with free information in English and Mandarin on the novel coronavirus COVID-19. The COVID-19 resource centre is hosted on Elsevier Connect, the company's public news and information website.

Biosensors and Bioelectronics 212 (2022) 114385

Contents lists available at ScienceDirect

Biosensors and Bioelectronics

journal homepage: www.elsevier.com/locate/bios

Nanoelectrokinetic-assisted lateral flow assay for COVID-19 antibody test

Cheonjung Kim [a,1], Yong Kyoung Yoo [b,1], Na Eun Lee [a,d], Junwoo Lee [a], Kang Hyeon Kim [a], Seungmin Lee [a,c], Jinhwan Kim [a], Seong Jun Park [a], Dongtak Lee [c], Sang Won Lee [c], Kyo Seon Hwang [e], Sung Il Han [f], Dongho Lee [f], Dae Sung Yoon [c,**], Jeong Hoon Lee [a,*]

[a] Department of Electrical Engineering, Kwangwoon University, Seoul, 01897, Republic of Korea
[b] Department of Electronic Engineering, Catholic Kwandong University, 24, Beomil-ro 579 beon-gil, Gangneung-si, Gangwon-do, 25601, Republic of Korea
[c] School of Biomedical Engineering, Korea University, Seoul, 02841, Republic of Korea
[d] Department of Biotechnology, College of Life Sciences and Biotechnology, Korea University, Seoul, 02841, Republic of Korea
[e] Department of Clinical Pharmacology and Therapeutics, College of Medicine, Kyung Hee University, Seoul, 02447, Republic of Korea
[f] CALTH Inc., Changeop-ro 54, Seongnam, Gyeonggi, 13449, Republic of Korea

ARTICLE INFO

Keywords:
Lateral flow assay
SARS-CoV-2 IgG
COVID-19
Self-testing
Biomarker
Preconcentration

ABSTRACT

A lateral flow assay (LFA) platform is a powerful tool for point-of-care testing (POCT), especially for self-testing. Although the LFA platform provides a simple and disposable tool for Coronavirus disease of 2019 (COVID-19) antigen (Ag) and antibody (Ab) screening tests, the lower sensitivity for low virus titers has been a bottleneck for practical applications. Herein, we report the combination of a microfluidic paper-based nanoelectrokinetic (NEK) preconcentrator and an LFA platform for enhancing the sensitivity and limit of detection (LOD). Biomarkers were electrokinetically preconcentrated onto a specific layer using the NEK preconcentrator, which was then coupled with LFA diagnostic devices for enhanced performance. Using this nanoelectrokinetic-assisted LFA (NEK-LFA) platform for self-testing, the severe acute respiratory syndrome coronavirus 2 Immunoglobulin G (SARS-CoV-2 IgG) sample was preconcentrated from serum samples. After preconcentration, the LOD of the LFA was enhanced by 32-fold, with an increase in analytical sensitivity (16.4%), which may offer a new opportunity for POCT and self-testing, especially in the COVID-19 pandemic and endemic global context.

1. Introduction

Lateral flow assays (LFAs) have demonstrated practical clinical utility as feasible point-of-care testing (POCT) platforms that satisfy most of the World Health Organization's ASSURED criteria (affordable, sensitive, specific, user-friendly, rapid/robust, equipment-free, and deliverable to end users) regarding many self-testing products (i.e., pregnancy, influenza A/B, and malaria diagnostic tests). Moreover, as LFAs use fluidic flow under capillary action, no external power equipment (e.g., pumps or centrifuges) is required for device operation. However, commercial LFAs have several limitations, including poorer sensitivity and lower specificity compared to those of laboratory tests (e.g., enzyme-linked immunosorbent assay (ELISA) and polymerase chain reaction (PCR)) (Carter et al., 2020; Udugama et al., 2020; van Kasteren et al., 2020; Wolfel et al., 2020).

Research is underway to improve the sensitivity and specificity of LFAs to achieve more accurate and high-performance POCT. Such investigations have primarily focused on assay optimization (reagent and receptor) (Dighe et al., 2022; Garg et al., 2021; Grant et al., 2020; Yu et al., 2020; Zhang et al., 2021), signal amplification (chemical enhancement and electrochemistry and fluorescence reader) (Cheng et al., 2017; Wang et al., 2017, 2021), and sample enrichment (magnetic separation and electrokinetic pre-concentration) (Kang et al., 2021; C. Wang et al., 2021; L. Wang et al., 2021; Zhou et al., 2021) to achieve high sensitivity and selectivity (Dempsey and Rathod, 2018 Han et al., 2020; Jia et al., 2018; Li et al., 2019; Loynachan et al., 2018; Mu et al., 2019; Niu et al., 2020, Niu et al., 2021; Ojaghi et al., 2018; Xu et al., 2014). As one of the sample enrichment techniques, our group described a nanoelectrokinetic (NEK)-based method for sample enrichment on paper, illustrating that bovine serum albumin (BSA) can be

* Corresponding author.
** Corresponding author.
E-mail addresses: dsyoon@korea.ac.kr (D.S. Yoon), jhlee@kw.ac.kr (J.H. Lee).
[1] These authors contributed equally.

https://doi.org/10.1016/j.bios.2022.114385
Received 21 February 2022; Received in revised form 8 May 2022; Accepted 14 May 2022
Available online 17 May 2022

preconcentrated by up to five times the initial concentration in serum (Han et al., 2018; Jeong et al., 2018). Further, this method was integrated with the commercial pregnancy LFA to increase the limit of detection (LOD) by 2.69-fold) and analytical sensitivity by 26%, illustrating a linear relationship between these variables (Kim et al., 2017). Most recently, we developed a large-volume preconcentrator (LVP) platform using the NEK concentration technology (Lee et al., 2021).

Severe acute respiratory syndrome coronavirus 2 (SARS-CoV-2) is currently spreading rapidly worldwide, and the WHO declared the coronavirus disease of 2019 (COVID-19) a pandemic on March 11, 2020 (Chinazzi et al., 2020; Liu et al., 2020; Menni et al., 2020; Salje et al., 2020; Tian et al., 2020; Zhang et al., 2020). In the beginning of 2022, the omicron variant became the dominant variant in many countries since it replicated faster than all other SARS-CoV-2 variants. In the pandemic and endemic period following expansion of the omicron variant, a highly sensitive LFA is an optimal candidate for companion diagnostics. For example, fast detection enables immediate treatment with antiviral drugs, such as Paxlovid, for COVID-19 via oral route. In addition, rapid and highly sensitive on-site serological assays to measure antibody levels during COVID-19 are extremely important for monitoring immunological responses to SARS-CoV-2 in various clinical environments. However, the general method incurs high costs due to the required manpower and equipment, leading to health care inequality in low-income countries (Orach, 2009).

To resolve this issue, an inexpensive POCT technology is required, and self-testing using paper based LFA has emerged as a promising technology. For example, our study confirmed the applicability of SARS-CoV-2 antibody diagnosis using an LFA. SARS-CoV-2 antibody testing could provide crucial information on convalescence from COVID-19, and will likely help determine the level of community immunity, especially in the endemic period after the rapid spread of the omicron variant. (Röltgen et al., 2020; Veldhoen and Simas, 2021). Enzyme-linked immunosorbent assay (ELISA), Automated Chemiluminescence Immunoassay (CLIA), LFA, and Microsphere immunoassay (MIA) can detect SARS-CoV-2 antibodies. The important characteristics of ELISA, CLIA, LFA, and MIA, including sample volume, test time, the potential for POCT, and others are described in Table S1. Among them, LFA was fast, inexpensive, and easy to use (optimal for POCT). However, this method has several limitations, including lower sensitivity and specificity than laboratory tests. The sensitivity of the SARS-CoV-2 LFA antibody test is 55% that of RT-PCR and 65% that of ELISA (Flower et al., 2020; Panel et al., 2020; Serrano et al., 2020; Theel et al., 2020).

In this study, the NEK preconcentrator was combined with an LFA platform to overcome the poor sensitivity and LOD of the LFA, as illustrated in Fig. 1. We designed the NEK-LFA to obtain an easy-to-implement form of LFA application and achieved an enrichment factor of >30-fold. The corresponding extraction efficiency of transferring the preconcentration plug onto the LFA was >90%. Moreover, we achieved enhanced sensitivity with increased LOD (~32-fold) for SARS-CoV-2 Immunoglobulin G (IgG).

2. Material and methods

2.1. Materials

Glass fiber-based composite paper (Whatman paper, fusion 5™, GE Healthcare Life Sciences, USA) was used to prepare paper materials. To test candidates for the collection disc, various types of paper were used including Whatman grade 1 ™, Whatman grade 6 ™, and Whatman fusion 5 ™. The other materials used in this study are as follows: orange-G color dye (Sigma-Aldrich, USA), 20 wt% Nafion resin (Sigma-Aldrich, USA), Alexa Fluor™ 594 conjugated albumin from bovine serum (BSA, Thermo Fisher Scientific, USA), SARS-CoV-2 antibody (sodium citrate plasma, Trina Bioreactives AG, Switzerland), Purfied anti-β-amyloid 1–16 antibody (6E10, BioLegend, USA), PAC-1 monoclonal antibody (Invitrogen, USA), CD42b monoclonal antibody (Invitrogen, USA), and a commercial SARS-CoV-2 IgG/IgM LFA kit (AllCheck COVID-19 IgG/IgM; Calth Co., Korea).

2.2. Development and operation of the rolling disc preconcentrator

Fig. 1 shows the overall procedure starting from assembly to operation of the device. Nafion cation exchange membranes were prepared

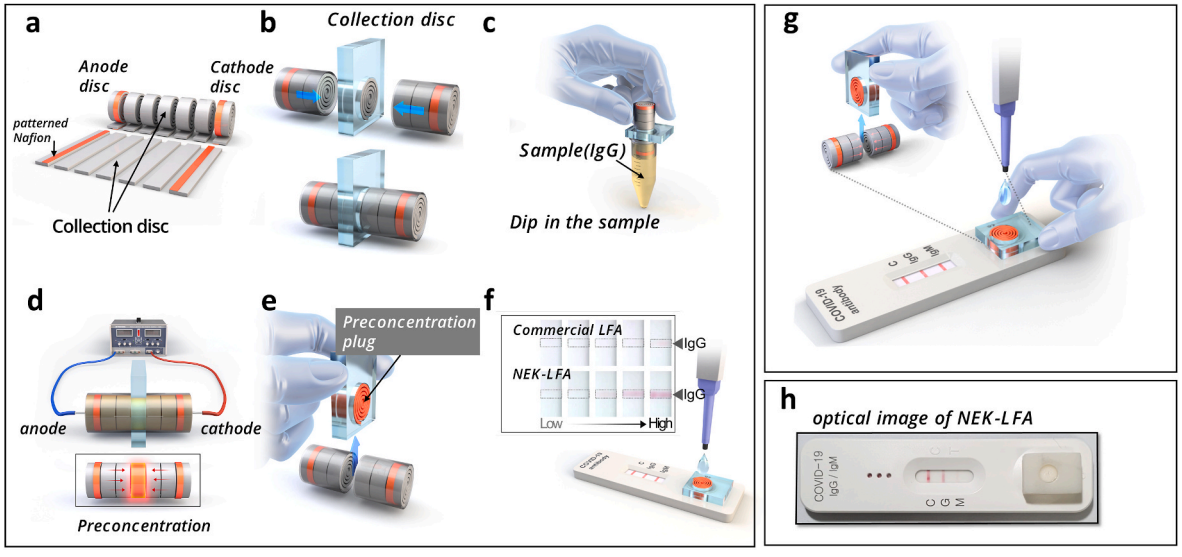

Fig. 1. The overall procedure of NEK preconcentration from assembly to LFA applications. (a) NEK-LFAs are prepared using Nafion coated cellulose paper and the collection disc. (b) To easily manipulate the preconcentrating target, the collection disc is located between the multilayered preconcentrator bodies. (c) The assembled NEK-LFA is immersed in the sample. (d) After removing the NEK-LFA from the sample, a voltage of 150 V is applied to generate ICP, and the SARS-CoV-2 antibody is preconcentrated on the collection disc. (e) The enriched SARS-CoV-2 antibody on the discs is recovered by simply removing the collection disc. (f) After placing the collection disc on sample inlet of the commercial LFA, elution buffer is injected, eliciting enhanced colorimetric signals. (g) The overall concept of the NEK-LFA. (h) Image of the SARS-CoV-2 antibody LFA kit carried out using the NEK-LFA. NEK-LFA, nanoelectrokinetic lateral flow assay; ICP, ion concentration polarization; SARS-CoV-2, severe acute respiratory syndrome coronavirus 2.

by drop-casting a Nafion resin onto rectangular paper specimens using a pipette and then drying the samples on a hot plate at 70 °C for 15 min. The Nafion film was coated along the breadth of the rectangular paper specimens, which were then rolled into discs (Fig. 1a). Subsequently, the these discs (two Nafion-coated discs and plain discs) were inserted and assembled in a three dimensional (3D)-printed case, as shown in Fig. 1b.

In Fig. 1c–f we show the entire process of preconcentration and LFA application with the NEK-LFA. The case containing the rolling discs was immersed in a biological sample for sample uptake into device (Fig. 1c). After sample injection into the rolling disc, a voltage was applied to both ends of the device to generate electrokinetic forces that concentrated the sample (IgG) on the central disc (collection disc) (Fig. 1d). Thereafter, the central collection disc with the concentrated sample was retrieved from the case (Fig. 1e) and coupled with the SARS-CoV-2 antibody kit. Then, an elution buffer was used to extract the concentrated sample. Fig. 1f demonstrates that the color (IgG line) of the LFA kit coupled with the collection disc was more intense compared with that of the kit without the collection disc. That is, the color intensity of the enriched sample was improved compared with that of the non-enriched one. Fig. 1h shows the optical image of the NEK-LFA at the sample extraction step (Fig. 1f). We designed a 3D printed device and used it to preconcentrate samples (Fig. S1).

2.3. Working principle

The working principle of the NEK preconcentration is described in our previous work (Lee et al., 2021). Briefly, when an electric field is applied across the NEK device, the ion concentration polarization (ICP) phenomenon occurs at the Nafion cation exchange membranes in the cathode and anode, and charged ions begin to move inside the paper channel. At the cathode, a depletion region is created by the overlap of the electrophoretic force and electric double layer generated by the Nafion membrane. Meanwhile, because positive ions are continuously introduced into the sample at the anode with the Nafion membrane, the concentrated plug moves to the center under the influence of an electroosmotic drag force. In contrast, negatively charged ions and biomolecules cannot move to the positive electrode of the cathode. Thus, by balancing the ICP electrokinetic forces, the sample can be preconcentrated around the central area (collection disc) (Fig. S2). After sample concentration using the ICP effect, the collection disc with concentrated biomolecules was coupled with the SARS-CoV-2 antibody kit for sample injection (Fig. S3).

2.4. Preparation of the SARS-CoV-2 antibody sample

To show the sensitivity and limit of detection (LOD) of the NEK-LFA, we prepared serum samples from a patient vaccinated with the Pfizer vaccine against COVID-19. Additionally, to demonstrate the sensitivity and LOD of the NEK-LFA versus a commercial LFA, we purchased a mixed vaccinated serum sample from Trina Bioreactives and prepared several concentrations starting at an IgG concentration of 217 arbitrary unit (AU)/mL (Fig. 4). Detailed Trina vaccinated IgG sample information is shown in Table S2. To maintain the ionic strength, the 12 concentrations we prepared were diluted with normal serum (Cat. S1-LITER, Merck Millipore, MA, USA) purchased prior to the COVID-19 outbreak.

Furthermore, we prepared the serum samples from a patient vaccinated with Moderna (COVID-19 vaccine panel G, Access Biologicals LLC, USA) to evaluate the method with another vaccine. Detailed sample information is shown in Table S3. From the panels, we prepared five samples from vaccinated patients to clearly demonstrate the efficacy of the NEK-LFA (Fig. 6). We included four low concentration samples which cannot be detected using a commercial LFA kit.

We designed experiments using single drop finger pricks (~40 μL) for self-test with both the NEK-LFA and commercial LFA. Following to the manufacturer's guideline, we used 10 μL samples for the commercial LFA test, then flowed ~100 μL of buffer solution on the device. For the NEK-LFA, we used 30 μL samples, which can be collected from finger pricks mixed with the buffers (270 μL, AllCheck COVID-19 IgG/IgM buffer; Calth Co., South Korea). Finally, the NEK preconcentration was carried out using 300 μL samples.

2.5. Analysis of the SARS-CoV-2 IgG antibody using SDS-PAGE

The concentrated IgG antibody was analyzed using sodium dodecyl sulfate–polyacrylamide gel electrophoresis (SDS-PAGE) (KOMA precast gel BC type, Koma Biotech, South Korea). The IgG antibody was mixed with a sample buffer consisting of native sample buffer (900 μL), 2-mercaptoethanol (200 μL), and SDS powder (8 mg). Then, 2.5 μL of the prepared sample buffer and 3.5 μL of distilled water were added to 4 μL of the concentrated IgG antibody. All the reagents were mixed thoroughly and heated at 100 °C for 15 min. A 10 μL volume of each sample was loaded onto the 6% polyacrylamide loading gel immersed in a running buffer. The running buffer consisted of 3.02 g of 25 mM Trizma base, 18.8 g of 250 mM glycine, 1 g of 0.2% SDS, and 1 L of distilled water. The 6% polyacrylamide gel was run for 45 min at 150 V. Subsequently, the gel was stained with Coomassie brilliant blue. Thereafter, de-staining was performed overnight in distilled water. The de-stained gel was analyzed using an LED gel illuminator (Table S4).

2.6. Fluorescence images and LFA color intensity analysis

All fluorescence images were acquired using a fluorescence microscope (IX-71, Olympus, Japan) equipped with a charge-coupled device camera (Hamamatsu Co., Japan). The fluorescence images were analyzed using the ImageJ software (Wayne Rasband, National Institute of Health, Bethesda, MD, USA).

The color intensity of the commercial LFA kit (SARS-CoV-2 IgG/IgM antibody kit) was analyzed using a custom-made imaging system operated using the LabVIEW software (National Instruments Co., USA) (see Fig. S4).

To set LOD values, we first measured color signals using the commercialized reader and custom-made National Instrument (NI) controlled optical system with the LabVIEW software. Next, five individually trained engineers (Calth Inc. http://www.thecalth.com) observed the colorimetric signal using the standard color chart and the manufacturer's guidelines to determine the LOD from the samples (positive/negative). Finally, we determined the LOD color intensity values in the reader/optical system using labeled information.

3. Results and discussion

3.1. NEK-LFA operation and concentrated plug extraction

To obtain a highly concentrated IgG antibody sample in a specific layer, the final position of the preconcentration plug should be preidentified for placing the collection disc in the device (Fig. 2). To determine the optimal position, we first examined the preconcentration of Orange G dye under four different voltages (30, 50, 100, and 150 V) using 0.1 × human serum. The Orange-G dye was used to track the enrichment process because it has a net negative charge and appears orange in aqueous solutions. To minimize dye adsorption due to nonspecific binding, we mixed 0.5% Tween 20 with 0.1 × serum (Fig. 2a). When the NEK-LFA was operated for 15 min, the movement of the Orange-G dye toward the center of the NEK preconcentrator was clearly observed. As the electrical voltage increased, the preconcentrating plugs gradually migrated to the central part of the NEK preconcentrator.

Further, under 150 V, the concentrated plug was located in a specific area (8–12 mm away from the left side of the NEK preconcentrator), and the highest color intensity appeared near the central part (~10 mm away from the left side of the NEK preconcentrator), as shown in Fig. 2b.

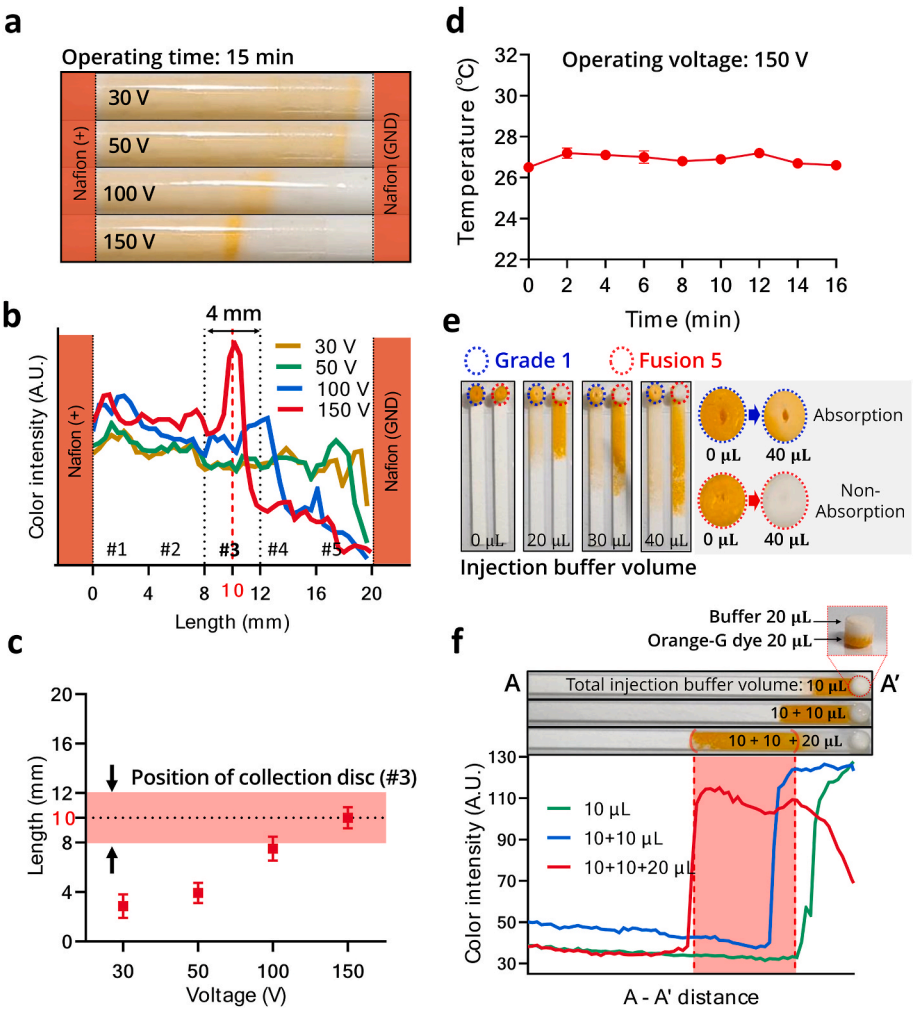

Fig. 2. Preconcentration and recovery of the Orange G dye using the NEK preconcentrator and its colorimetric analysis. (a) The Orange G dye is preconcentrated under different voltages and the preconcentrating plugs gradually migrated to the central part of the NEK preconcentrator device with increasing voltages. (b) Under 150 V, the positions of the highest peaks are near the center. (c) The highest color intensity appeared near the central part (10 mm away from the left side) where the collection disc is located. (d) Temperature measurement during the entire preconcentration time. The temperature rise was negligible (<1.5 °C, measurements repeated thrice). (e–f) The feasibility of transferring the preconcentration plug into the LFA kit. We sequentially eluted the collection disc with buffer, indicating that the enriched sample could be seamlessly transferred to the LFA kit. NEK, nanoelectrokinetic; LFA, lateral flow assay.

Finally, the location with high color intensity, where the dye was highly concentrated (disc #3 in Fig. 2c) was selected as the collection disc. For clearer observation, a very high dye concentration was used in this experiment; therefore, a fraction of the dye remained along the path of its movement. This issue could however be prevented using an optimized sample concentration.

We confirmed that the target sample remained intact because the sample did not contact the electrodes. Moreover, we applied a moderate electric field (~70 V/cm) to the NEK preconcentrator, which is much lower than that used in conventional capillary electrophoresis (>300 V/cm). We also verified that the temperature increase due to the electric current (operating voltage: 150 V) was negligible (<1.5 °C), as shown in Fig. 2d. This ensures that no denaturation or degradation of the SARS-CoV-2 IgG antibody occurs during preconcentration, which was also verified through SDS-PAGE and LFA tests.

One of the important parameters of our NEK pre-concentrator is the extraction efficiency of the preconcentrated plug. The preconcentrated biomolecule should be effectively extracted from the collection disc with minimized loss and absorption. To visualize the extraction efficiency, we used the Orange-G dye for tracking the extraction process. To check the feasibility of transferring the preconcentration plug into the LFA kit, we sequentially eluted the collection disc with 10 µL aliquots of buffer and monitored the movement of the extraction plug over time (Fig. 2e). The results indicated that the enriched sample could be seamlessly transferred to the LFA kit with a well-defined preconcentrated plug (Fig. 2f). Further, we evaluated collection discs made using several different paper types (Whatman Fusion 5, Grade 6, and Grade 1). Among them, Whatman Fusion 5™ paper exhibited less adsorption of biomolecules and high recovery (Fig. 3c).

3.2. Protein preconcentration and extraction test

After evaluating the preconcentration and extraction properties of the NEK preconcentrator via Orange-G dye, we evaluated it with a protein sample, BSA labeled with Alexa 594. In Fig. 3a we showed the concentrated plug with fluorescence images, revealing that the BSA was enriched and spatially confined in disc #3, where the collection disc was located. After disassembly (Fig. 3a), we also monitored each disc using 3D fluorescence images to extract the concentrated plug. Following the preconcentration time, the position (~10 mm) of the highest intensity peak was observed near the center (Fig. 3b). We verified that, in 15 min, the final location of the enriched plug was within 8–12 mm of the electrode, where the collection disc was inserted,. After 15 min under 150 V, we achieved an enrichment factor of >30, as indicated by the fluorescence intensity. After the extraction process, the enriched discs showed much lower fluorescence intensities (Fig. 3c), indicating that the concentrated BSA was efficiently extracted from the collection disc. We evaluated the extraction efficiency using the ratio of the released sample intensity to the injected sample intensity of the 594-BSA used in the extraction process. The extraction efficiencies were 95.7, 37, and 17.2% for Whatman Fusion 5, Grade 6, and Grade 1 paper, respectively (Table S5). Based on the extraction efficiency, we used Whatman Fusion 5™ paper for assembling the collection discs (Fig. 1b).

Next, we conducted the SDS-PAGE analysis of the SARS-CoV-2 IgG

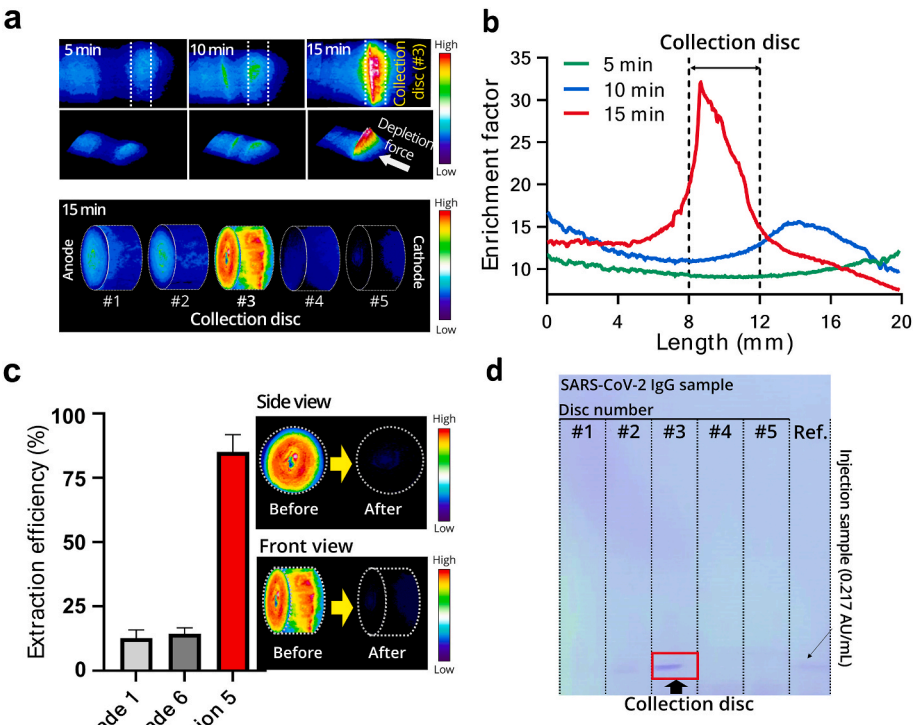

Fig. 3. Preconcentration and recovery of BSA and SARS-CoV-2 IgG antibody. (a) Fluorescence 3D images of BSA during preconcentration. After 15 min concentration, the enriched BSA is located on layer 3 (collection disc). (b) An enrichment factor above 30 was acquired using BSA proteins. (c) The extraction efficiencies were 95.7, 37, and 17.2% for Whatman Fusion 5, Grade 6, and Grade 1 paper, showing Whatman Fusion 5™ paper is the best candidate for fabricating the collection disc. (d) SDS-PAGE analysis of the SARS-CoV-2 IgG antibody after the NEK-LFA, showing the enhanced signals only in layer 3 (collection disc). BSA, bovine serum albumin; 3D, three dimensional; SDS-PAGE, sodium dodecyl sulfate–polyacrylamide gel electrophoresis; NEK-LFA, nanoelectrokinetic lateral flow assay; ICP, ion concentration polarization; SARS-CoV-2, severe acute respiratory syndrome coronavirus 2.

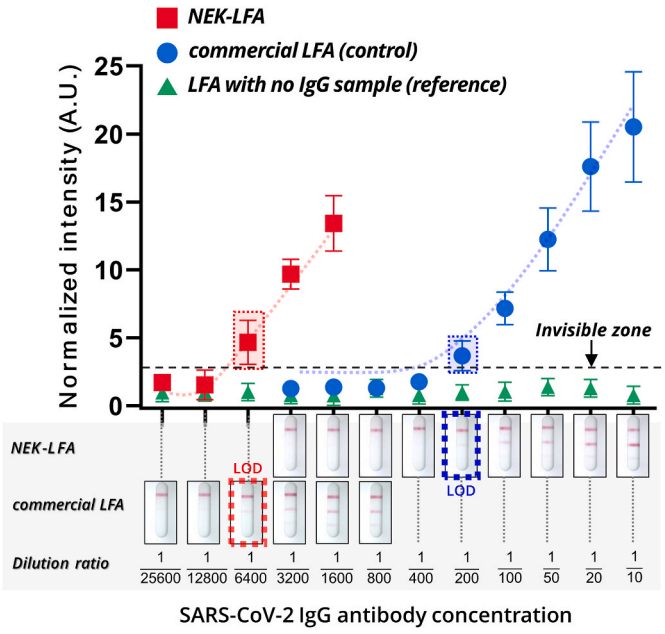

Fig. 4. The LOD and sensitivity of the NEK-LFA were enhanced (~32 increase and 16.4% increase, respectively) compared with the commercial LFA. We used the serum samples from a person vaccinated with Pfizer and prepared 12 concentrations. For the control experiment, we used the commercialized SARS-CoV-2 IgG LFA. NEK-LFA, nanoelectrokinetic lateral flow assay; IgG, immunoglobulin G; SARS-CoV-2, severe acute respiratory syndrome coronavirus 2; AU, arbitrary unit.

antibody preconcentrated using the NEK-LFA. We started with 0.217 AU/mL of the IgG reference sample and observed the highest color intensity only on disc #3, implying that the use of the NEK-enhanced LFA can significantly improve downstream assays, such as the LFA (Fig. 3d).

3.3. Sensitivity and LOD enhancement of the SARS-CoV-2 antibody

We analyzed the effect of the NEK-LFA on the commercial COVID-19 antibody LFA kit. For this, we prepared 13 different sample concentrations (1, 1/10, 1/20, 1/50, 1/100, 1/200, 1/400, 1/800, 1/1600, 1/3200, 1/6400, 1/12800, and 1/25600 on 1 × basis, 217 AU/mL) and used a commercial SARS-CoV-2 (COVID-19) IgG/IgM antibody kit. Fig. 4 shows the sensitivity and LOD enhancement facilitated by the NEK-LFA.

For control experiments, we tested the commercial SARS-CoV-2 IgG/IgM antibody kit. The color intensities of the test and control lines were analyzed using a custom-built imaging system operated using the LabVIEW™ software (Fig. S3). The colorimetric intensity was normalized to determine the LOD (Fig. 4a). For the references, we prepared the commercialized SARS-CoV-2 IgG/IgM antibody kit, then assayed it using a buffer-only solution without IgG targets. All assays were carried out ten times to verify the reproducibility. To calculate the analytical LOD, we used the following equation (Armbruster and Pry, 2008).

$$Opticalintensity_{LOD} = blank_{TL} + 3\sigma_{blank} \quad (1)$$

Fig. 4a shows the normalized colorimetric intensity versus SARS-CoV-2 antibody concentration plot obtained without the NEK-assisted enrichment process. The analysis of the color intensity without the NEK-LFA yielded an LOD of 1/200 concentration. Meanwhile, we observed signals at 1/6400 concentration, corresponding to a 32-fold increase in the LOD with the NEK-LFA enrichment process. We hypothesize that the NEK-assisted enrichment process can increase the entropy, leading to an exponential decrease in the dissociation constant, resulting in increased binding affinity, which can enhance both the sensitivity and LOD of immunoassays (Yoo et al., 2017).

The slope of the color intensity versus concentration plot indicates the analytical sensitivity., The NEK-LFA showed a relatively high slope (~16.4% increase) with a higher LOD (~32-fold) than the LFA without preconcentration demonstrating the great potential of the NEK-assisted enrichment process for POCT. In addition, the NEK-assisted enrichment process can be used to concentrate samples of different dilutions by simply increasing the volume of the NEK preconcentrator, which can

enhance the performance of LFAs.

3.4. SARS-CoV-2 antibody specificity test

To conduct the LFA using an electric field or by changing specific external conditions, it is necessary to verify whether specific binding causes the test line color. We suspected that pH changes during the NEK-assisted preconcentration process may change the specificity of the antigen–antibody interaction or cause protein denaturation. To examine the specificity, we tested six different conditions. First, we evaluated the effect of NEK preconcentration on the LFA. Starting with 1/6400 sample concentration, we performed NEK preconcentration and showed clear strong positive signals after the LFA. However, we observed negative signals without the NEK-LFA. Second, to further examine whether non-specific binding happens after NEK-assisted preconcentration, we tested the PAC-1 monoclonal antibody, CD42b monoclonal antibody, anti-β-amyloid (6E10) antibody and observed no LFA signals. Finally, we confirmed no LFA signals from the BSA and buffer only sample after NEK-assisted preconcentration (Fig. 5).

3.5. Ability of extending the NEK-LFA LOD using samples from Moderna vaccinated patients

In the previous section, we validated the NEK-LFA using serum samples from a patient vaccinated with the Pfizer vaccine against COVID-19. While we successfully demonstrated the efficacy of the NEK-LFA with these samples, we sought to verify if the NEK-LFA LOD could be extended using an undiluted sample from another vaccinated patient. Also, samples from patients vaccinated with the Moderna vaccine against COVID-19 enabled crosschecking the efficacy of the assay to detect antibodies derived from alternative immunization methods. We prepared five samples to thoroughly evaluate the performance of the NEK-assisted LFA (Fig. 6). We included four low concentration samples to validate the performance of the NEK-LFA since the commercial LFA cannot detect those low IgG concentrations, which can.

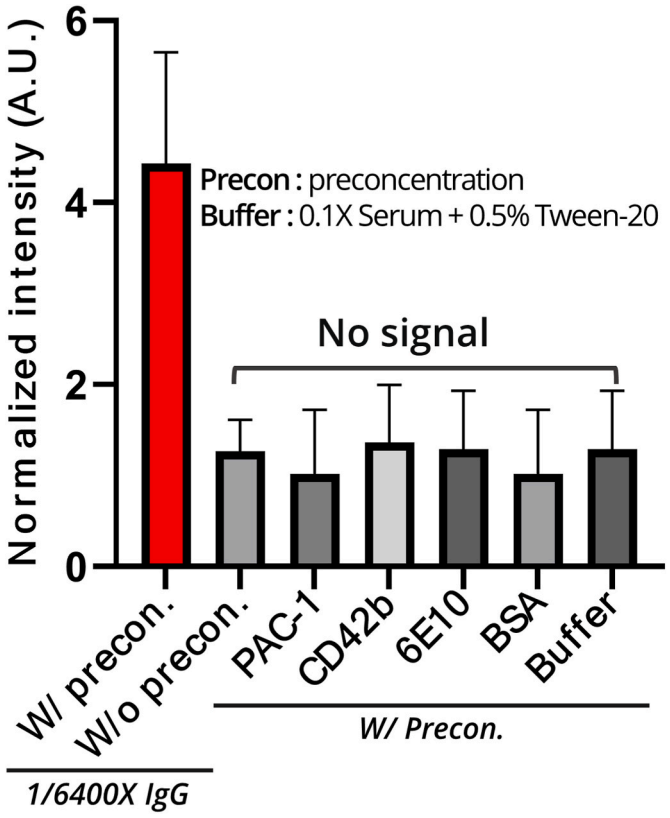

Fig. 5. Specificity test of the NEK-LFA. We tested six different samples for specificity and cross-reactivity in NEK-LFA. Positive control: with NEK preconcentration (red bar), Specificity test 1) without NEK preconcentration, 2) PAC-1 monoclonal antibody, 3) CD42b monoclonal antibody, 4) anti-amyloid (6E10), 5) bovine serum albumin (BSA), and 6) buffer only. NEK-LFA, nanoelectrokinetic lateral flow assay; IgG, immunoglobulin G; SARS-CoV-2, severe acute respiratory syndrome coronavirus 2; Precon., Preconcentration; IgG, immunoglobulin G; W/, with; W/o, without; BSA, bovine serum albumin; AU, arbitrary unit.

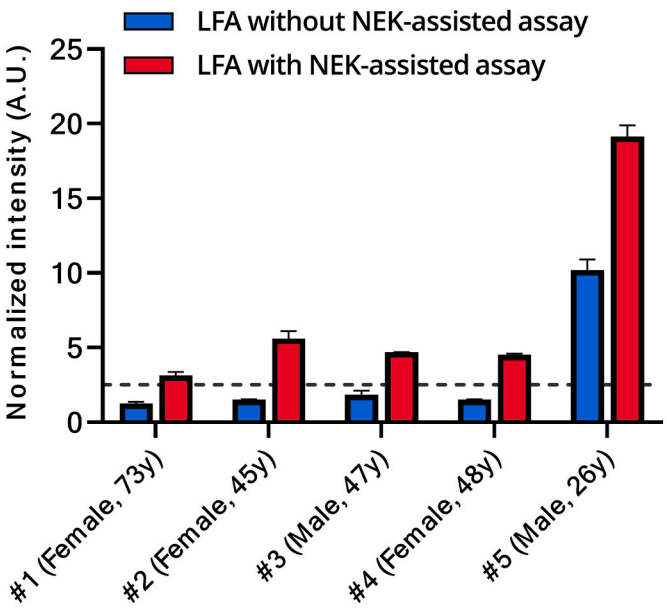

Fig. 6. Crosscheck the ability of the NEK-LFA to detect antibodies in samples from patients vaccinated with the Moderna vaccine against COVID-19. We prepared five samples including four low concentration samples below the LOD of the commercial LFA, validating the extended sensitivity and LOD of the NEK-LFA. NEK-LFA, nanoelectrokinetic lateral flow assay; COVID-19, coronavirus disease of 2019; LOD, limit of detection; AU, arbitrary unit.

As mentioned, among five samples, four [#1 (female, 73 years of age), #2 (female, 45 years of age), #3 (male, 47 years of age), and #4 (female, 48 years of age)] had low concentrations and elicited no colorimetric signal in the commercial LFA since the concentrations of samples were below the commercial LFA LOD. We increased the colorimetric signal with the NEK-LFA by concentrating target samples and enhanced the LOD by adapting the preconcentrating step. For patient #5 (male, 26 years of age) the samples were detectable using the commercial LFA. Nonetheless, we also strongly enhanced the colorimetric signal for these samples, indicating the ability to extend the sensitivity and LOD of the NEK-LFA with human serum samples.

4. Conclusions

We have developed a novel platform for a NEK-LFA with enhanced performance. We designed and optimized a paper-based device to concentrate proteins at specific locations with a balanced electrokinetic force. Using the preconcentration platform, the proteins, including SARS-CoV-2 IgG/IgM antibodies, were concentrated to more than 30-times the initial concentration. In addition, the enhanced analytical sensitivity (~16.4% increase) combined with the increased LOD (~32-fold) of the NEK-LFA highlights the potential of this assay for POCT. Compared with the commercial LFA, our preconcentration platform affords outstanding biomarker enrichment that may be applied for highly sensitive POCT. This LFA is a promising candidate for POCT in the COVID-19 pandemic and endemic period, and we believe that our platform provides a highly sensitive POCT with simplicity and high performance. Ongoing studies are optimizing the NEK-LFA platform for

a salivary sample assay similar to the OraQuick advance rapid HIV-1/2 antibody test.

CRediT authorship contribution statement

Cheonjung Kim: Conceptualization, Methodology, Investigation, Formal analysis, Writing – review & editing. **Yong Kyoung Yoo:** Methodology, Validation, Formal analysis, Writing – review & editing. **Na Eun Lee:** Formal analysis, Investigation. **Junwoo Lee:** Methodology, Formal analysis. **Kang Hyeon Kim:** Software. **Seungmin Lee:** Formal analysis. **Jinhwan Kim:** Data curation. **Seong Jun Park:** Data curation. **Dongtak Lee:** Formal analysis, Visualization. **Sang Won Lee:** Software. **Kyo Seon Hwang:** Writing – review & editing. **Sung Il Han :** Resources. **Dongho Lee :** Resources. **Dae Sung Yoon:** Supervision, Writing – review & editing. **Jeong Hoon Lee:** Conceptualization, Supervision, Project administration, Writing – review & editing.

Declaration of competing interest

The authors declare that they have no known competing financial interests or personal relationships that could have appeared to influence the work reported in this paper.

Acknowledgment

This research was supported by the Bio & Medical Technology Development Program of the National Research Foundation (NRF) funded by the Korean government (MSIT) (No. 2021M3E5E3080743). The work reported in this paper was conducted during the sabbatical year of Kwangwoon University in 2022.

Appendix A. Supplementary data

Supplementary data to this article can be found online at https://doi.org/10.1016/j.bios.2022.114385.

References

Armbruster, D.A., Pry, T., 2008. Limit of blank, limit of detection and limit of quantitation. Clin. Biochem. Rev. 29, S49–S52. Suppl 1(Suppl 1).

Carter, L.J., Garner, L.V., Smoot, J.W., Li, Y., Zhou, Q., Saveson, C.J., Sasso, J.M., Gregg, A.C., Soares, D.J., Beskid, T.R., Jervey, S.R., Liu, C., 2020. Assay techniques and test development for COVID-19 diagnosis. ACS Cent. Sci. 6 (5), 591–605.

Cheng, Z., Choi, N., Wang, R., Lee, S., Moon, K.C., Yoon, S.-Y., Chen, L., Choo, J., 2017. Simultaneous detection of dual prostate specific antigens using surface-enhanced Raman scattering-based immunoassay for accurate diagnosis of prostate cancer. ACS Nano 11 (5), 4926–4933.

Chinazzi, M., Davis, J.T., Ajelli, M., Gioannini, C., Litvinova, M., Merler, S., Piontti, A.P. y., Mu, K., Rossi, L., Sun, K., Viboud, C., Xiong, X., Yu, H., Halloran, M.E., Longini, I. M., Vespignani, A., 2020. The effect of travel restrictions on the spread of the 2019 novel coronavirus (COVID-19) outbreak. Science 368 (6489), 395–400.

Dempsey, E., Rathod, D., 2018. Disposable printed lateral flow electrochemical immunosensors for human cardiac troponin T. IEEE Sensor. J. 18 (5), 1828–1834.

Dighe, K., Moitra, P., Alafeef, M., Gunaseelan, N., Pan, D., 2022. A rapid RNA extraction-free lateral flow assay for molecular point-of-care detection of SARS-CoV-2 augmented by chemical probes. Biosens. Bioelectron. 200, 113900.

Flower, B., Brown, J.C., Simmons, B., Moshe, M., Frise, R., Penn, R., Kugathasan, R., Petersen, C., Daunt, A., Ashby, D., Riley, S., Atchison, C.J., Taylor, G.P., Satkunarajah, S., Naar, L., Klaber, R., Badhan, A., Rosadas, C., Khan, M., Fernandez, N., Sureda-Vives, M., Cheeseman, H.M., O'Hara, J., Fontana, G., Pallett, S.J.C., Rayment, M., Jones, R., Moore, L.S.P., McClure, M.O., Cherepanov, P., Tedder, R., Ashrafian, H., Shattock, R., Ward, H., Darzi, A., Elliot, P., Barclay, W.S., Cooke, G.S., 2020. Clinical and laboratory evaluation of SARS-CoV-2 lateral flow assays for use in a national COVID-19 seroprevalence survey. Thorax 75 (12), 1082–1088.

Garg, M., Sharma, A.L., Singh, S., 2021. Advancement in biosensors for inflammatory biomarkers of SARS-CoV-2 during 2019–2020. Biosens. Bioelectron. 171, 112703.

Grant, B.D., Anderson, C.E., Williford, J.R., Alonzo, L.F., Glukhova, V.A., Boyle, D.S., Weigl, B.H., Nichols, K.P., 2020. SARS-CoV-2 coronavirus nucleocapsid antigen-detecting half-strip lateral flow assay toward the development of point of care tests using commercially available reagents. Anal. Chem. 92 (16), 11305–11309.

Han, S.I., Yoo, Y.K., Lee, J., Kim, C., Lee, K., Lee, T.H., Kim, H., Yoon, D.S., Hwang, K.S., Kwak, R., Lee, J.H., 2018. High-ionic-strength pre-concentration via ion concentration polarization for blood-based biofluids. Sensor. Actuator. B Chem. 268, 485–493.

Han, G.-R., Ki, H., Kim, M.-G., 2020. Automated, universal, and mass-producible paper-based lateral flow biosensing platform for high-performance point-of-care testing. ACS Appl. Mater. Interfaces 12 (1), 1885–1894.

Jeong, D., Kim, J., Chae, M.-S., Lee, W., Yang, S.-H., Kim, Y., Kim, S.M., Lee, J.S., Lee, J. H., Choi, J., Yoon, D.S., Hwang, K.S., 2018. Multifunctionalized reduced graphene oxide biosensors for simultaneous monitoring of structural changes in amyloid-β 40. Sensors 18 (6), 1738.

Jia, X., Wang, C., Rong, Z., Li, J., Wang, K., Qie, Z., Xiao, R., Wang, S., 2018. Dual dye-loaded Au@Ag coupled to a lateral flow immunoassay for the accurate and sensitive detection of Mycoplasma pneumoniae infection. RSC Adv. 8 (38), 21243–21251.

Kang, J., Jang, H., Yeom, G., Kim, M.-G., 2021. Ultrasensitive detection platform of disease biomarkers based on recombinase polymerase amplification with H-sandwich aptamers. Anal. Chem. 93 (2), 992–1000.

Kim, C., Yoo, Y.K., Han, S.I., Lee, J., Lee, D., Lee, K., Hwang, K.S., Lee, K.H., Chung, S., Lee, J.H., 2017. Battery operated preconcentration-assisted lateral flow assay. Lab Chip 17 (14), 2451–2458.

Lee, D., Lee, J.W., Kim, C., Lee, D., Chung, S., Yoon, D.S., Lee, J.H., 2021. Highly efficient and scalable biomarker preconcentrator based on nanoelectrokinetics. Biosens. Bioelectron. 176, 112904.

Li, X., Yang, T., Song, Y., Zhu, J., Wang, D., Li, W., 2019. Surface-enhanced Raman spectroscopy (SERS)-based immunochromatographic assay (ICA) for the simultaneous detection of two pyrethroid pesticides. Sensor. Actuator. B Chem. 283, 230–238.

Liu, Y., Ning, Z., Chen, Y., Guo, M., Liu, Y., Gali, N.K., Sun, L., Duan, Y., Cai, J., Westerdahl, D., Liu, X., Xu, K., Ho, K.-f., Kan, H., Fu, Q., Lan, K., 2020. Aerodynamic analysis of SARS-CoV-2 in two Wuhan hospitals. Nature 582 (7813), 557–560.

Loynachan, C.N., Thomas, M.R., Gray, E.R., Richards, D.A., Kim, J., Miller, B.S., Brookes, J.C., Agarwal, S., Chudasama, V., McKendry, R.A., Stevens, M.M., 2018. Platinum nanocatalyst amplification: redefining the gold standard for lateral flow immunoassays with ultrabroad dynamic range. ACS Nano 12 (1), 279–288.

Menni, C., Valdes, A.M., Freidin, M.B., Sudre, C.H., Nguyen, L.H., Drew, D.A., Ganesh, S., Varsavsky, T., Cardoso, M.J., El-Sayed Moustafa, J.S., Visconti, A., Hysi, P., Bowyer, R.C.E., Mangino, M., Falchi, M., Wolf, J., Ourselin, S., Chan, A.T., Steves, C. J., Spector, T.D., 2020. Real-time tracking of self-reported symptoms to predict potential COVID-19. Nat. Med. 26 (7), 1037–1040.

Mu, X.-H., Liu, H.-F., Tong, Z.-Y., Du, B., Liu, S., Liu, B., Liu, Z.-W., Gao, C., Wang, J., Dong, H., 2019. A new rapid detection method for ricin based on tunneling magnetoresistance biosensor. Sensor. Actuator. B Chem. 284, 638–649.

Niu, J., Shi, H., Wei, H., Gao, B., Li, J.X., Xu, F., Li, X., Li, F., 2020. Liquid plasticine integrated with isoelectric focusing for miniaturized protein analysis. Anal. Chem. 92 (13), 9048–9056.

Niu, J., Bao, Z., Wei, Z., Li, J.X., Gao, B., Jiang, X., Li, F., 2021. A three-dimensional paper-based isoelectric focusing device for direct analysis of proteins in physiological samples. Anal. Chem. 93 (8), 3959–3967.

Ojaghi, A., Pallapa, M., Tabatabaei, N., Rezai, P., 2018. High-sensitivity interpretation of lateral flow immunoassays using thermophotonic lock-in imaging. Sensor Actuator Phys. 273, 189–196.

Orach, C.G., 2009. Health equity: challenges in low income countries. Afr. Health Sci. 9, S49–S51. Suppl 2(Suppl 2).

Panel, N.C.T.S.A., Adams, E.R., Ainsworth, M., Anand, R., Andersson, M.I., Auckland, K., Baillie, J.K., Barnes, E., Beer, S., Bell, J., Berry, T., Bibi, S., Carroll, M., Chinnakannan, S., Clutterbuck, E., Cornall, R.J., Crook, D.W., De Silva, T., Dejnirattisai, W., Dingle, K.E., Dold, C., Espinosa, A., Eyre, D.W., Farmer, H., Fernandez Mendoza, M., Georgiou, D., Hoosdally, S.J., Hunter, A., Jeffrey, K., Klenerman, P., Knight, J., Knowles, C., Kwok, A.J., Leuschner, U., Levin, R., Liu, C., Lopez-Camacho, C., Martinez Garrido, J.C., Matthews, P.C., McGivern, H., Mentzer, A.J., Milton, J., Mongkolsapaya, J., Moore, S.C., Oliveira, M.S., Pereira, F., Perez Lopez, E., Peto, T., Ploeg, R.J., Pollard, A., Prince, T., Roberts, D.J., Rudkin, J. K., Sanchez, V., Screaton, G.R., Semple, M.G., Skelly, D.T., Slon-Campos, J., Smith, E. N., Sobrino Diaz, A.J., Staves, J., Stuart, D., Supasa, P., Surik, T., Thraves, H., Tsang, P., Turtle, L., Walker, A.S., Wang, B., Washington, C., Watkins, N., Whitehouse, J., 2020. Antibody Testing for COVID-19: A Report from the National COVID Scientific Advisory Panel. medRxiv, 2020.2004.2015.20066407.

Röltgen, K., Powell, A.E., Wirz, O.F., Stevens, B.A., Hogan, C.A., Najeeb, J., Hunter, M., Wang, H., Sahoo, M.K., Huang, C., Yamamoto, F., Manohar, M., Manalac, J., Otrelo-Cardoso, A.R., Pham, T.D., Rustagi, A., Rogers, A.J., Shah, N.H., Blish, C.A., Cochran, J.R., Jardetzky, T.S., Zehnder, J.L., Wang, T.T., Narasimhan, B., Gombar, S., Tibshirani, R., Nadeau, K.C., Kim, P.S., Pinsky, B.A., Boyd, S.D., 2020. Defining the features and duration of antibody responses to SARS-CoV-2 infection associated with disease severity and outcome. Sci. Immunol. 5 (54), eabe0240.

Salje, H., Kiem, C.T., Lefrancq, N., Courtejoie, N., Bosetti, P., Paireau, J., Andronico, A., Hozé, N., Richet, J., Dubost, C.-L., Strat, Y.L., Lessler, J., Levy-Bruhl, D., Fontanet, A., Opatowski, L., Boelle, P.-Y., Cauchemez, S., 2020. Estimating the burden of SARS-CoV-2 in France. Science 369 (6500), 208–211.

Serrano, M.M., Rodríguez, D.N., Palop, N.T., Arenas, R.O., Córdoba, M.M., Mochón, M.D. O., Cardona, C.G., 2020. Comparison of commercial lateral flow immunoassays and ELISA for SARS-CoV-2 antibody detection. J. Clin. Virol. 129, 104529.

Theel, E.S., Slev, P., Wheeler, S., Couturier, M.R., Wong, S.J., Kadkhoda, K., 2020. The role of antibody testing for SARS-CoV-2: is there one? J. Clin. Microbiol. 58 (8).

Tian, H., Liu, Y., Li, Y., Wu, C.-H., Chen, B., Kraemer, M.U.G., Li, B., Cai, J., Xu, B., Yang, Q., Wang, B., Yang, P., Cui, Y., Song, Y., Zheng, P., Wang, Q., Bjornstad, O.N., Yang, R., Grenfell, B.T., Pybus, O.G., Dye, C., 2020. An investigation of transmission control measures during the first 50 days of the COVID-19 epidemic in China. Science 368 (6491), 638–642.

Udugama, B., Kadhiresan, P., Kozlowski, H.N., Malekjahani, A., Osborne, M., Li, V.Y.C., Chen, H., Mubareka, S., Gubbay, J.B., Chan, W.C.W., 2020b. Diagnosing COVID-19: the disease and tools for detection. ACS Nano 14 (4), 3822–3835.

van Kasteren, P.B., van der Veer, B., van den Brink, S., Wijsman, L., de Jonge, J., van den Brandt, A., Molenkamp, R., Reusken, C., Meijer, A., 2020. Comparison of seven commercial RT-PCR diagnostic kits for COVID-19. J. Clin. Virol. 128, 104412.

Veldhoen, M., Simas, J.P., 2021. Endemic SARS-CoV-2 will maintain post-pandemic immunity. Nat. Rev. Immunol. 21 (3), 131–132.

Wang, X., Choi, N., Cheng, Z., Ko, J., Chen, L., Choo, J., 2017. Simultaneous detection of dual nucleic acids using a SERS-based lateral flow assay biosensor. Anal. Chem. 89 (2), 1163–1169.

Wang, C., Shi, D., Wan, N., Yang, X., Liu, H., Gao, H., Zhang, M., Bai, Z., Li, D., Dai, E., Rong, Z., Wang, S., 2021a. Development of spike protein-based fluorescence lateral flow assay for the simultaneous detection of SARS-CoV-2 specific IgM and IgG. Analyst 146 (12), 3908–3917.

Wang, L., Wang, X., Cheng, L., Ding, S., Wang, G., Choo, J., Chen, L., 2021b. SERS-based test strips: principles, designs and applications. Biosens. Bioelectron. 189, 113360.

Wolfel, R., Corman, V.M., Guggemos, W., Seilmaier, M., Zange, S., Muller, M.A., Niemeyer, D., Jones, T.C., Vollmar, P., Rothe, C., Hoelscher, M., Bleicker, T., Brunink, S., Schneider, J., Ehmann, R., Zwirglmaier, K., Drosten, C., Wendtner, C., 2020. Virological assessment of hospitalized patients with COVID-2019. Nature 581 (7809), 465–469.

Xu, H., Chen, J., Birrenkott, J., Zhao, J.X., Takalkar, S., Baryeh, K., Liu, G., 2014. Gold-nanoparticle-decorated silica nanorods for sensitive visual detection of proteins. Anal. Chem. 86 (15), 7351–7359.

Yoo, Y.K., Yoon, D.S., Kim, G., Kim, J., Han, S.I., Lee, J., Chae, M.-S., Lee, S.-M., Lee, K. H., Hwang, K.S., Lee, J.H., 2017. An enhanced platform to analyse low-affinity amyloid β protein by integration of electrical detection and preconcentrator. Sci. Rep. 7 (1), 14303.

Yu, S., Nimse, S.B., Kim, J., Song, K.-S., Kim, T., 2020. Development of a lateral flow strip membrane assay for rapid and sensitive detection of the SARS-CoV-2. Anal. Chem. 92 (20), 14139–14144.

Zhang, J., Litvinova, M., Liang, Y., Wang, Y., Wang, W., Zhao, S., Wu, Q., Merler, S., Viboud, C., Vespignani, A., Ajelli, M., Yu, H., 2020. Changes in contact patterns shape the dynamics of the COVID-19 outbreak in China. Science 368 (6498), 1481–1486.

Zhang, C., Zheng, T., Wang, H., Chen, W., Huang, X., Liang, J., Qiu, L., Han, D., Tan, W., 2021. Rapid one-pot detection of SARS-CoV-2 based on a lateral flow assay in clinical samples. Anal. Chem. 93 (7), 3325–3330.

Zhou, Y., Wu, Y., Ding, L., Huang, X., Xiong, Y., 2021. Point-of-care COVID-19 diagnostics powered by lateral flow assay. Trac. Trends Anal. Chem. 145, 116452.